W/SiC x-ray multilayers optimized for use above 100 keV

David L. Windt, Soizik Donguy, Charles J. Hailey, Jason Koglin, Veijo Honkimaki, Eric Ziegler, Finn E. Christensen, Hubert Chen, Fiona A. Harrison, and William W. Craig

We have developed a new depth-graded multilayer system comprising W and SiC layers, suitable for use as hard x-ray reflective coatings operating in the energy range 100–200 keV. Grazing-incidence x-ray reflectance at $E = 8$ keV was used to characterize the interface widths, as well as the temporal and thermal stability in both periodic and depth-graded W/SiC structures, whereas synchrotron radiation was used to measure the hard x-ray reflectance of a depth-graded multilayer designed specifically for use in the range $E \sim 150$–170 keV. We have modeled the hard x-ray reflectance using newly derived optical constants, which we determined from reflectance versus incidence angle measurements also made using synchrotron radiation, in the range $E = 120$–180 keV. We describe our experimental investigation in detail, compare the new W/SiC multilayers with both W/Si and W/B_4C films that have been studied previously, and discuss the significance of these results with regard to the eventual development of a hard x-ray nuclear line telescope. © 2003 Optical Society of America

OCIS codes: 340.7470, 230.4170, 310.6860, 350.1260.

1. Introduction

Depth-graded x-ray multilayer mirrors are the enabling technology for a new generation of astronomical space telescopes operating above $E = 10$ keV, including the High-Energy Focusing Telescope (HEFT)[1] and In-Focus[2] balloon instruments and the Astro-G and Constellation-X satellite instruments.[3] The multilayer coatings are designed to provide broadband x-ray reflectance at grazing incidence. They are deposited onto lightweight cylindrical mirror substrates (such as thermally formed glass[4]) that are then mounted into a highly nested Wolter-type telescope geometry, thus providing subarcminute angular resolution and large effective area over a wide energy band.

D. L. Windt (windt@astro.columbia.edu), S. Donguy, C. J. Hailey, and J. Koglin are with the Columbia Astrophysics Laboratory, 550 West 120 Street, New York, New York 10027. V. Honkimaki and E. Ziegler are with the European Synchrotron Radiation Facility, Grenoble, France. F. E. Christensen is with the Danish Space Research Institute, 30 Juliane Maries Vej, 2100 Copenhagen, Denmark. H. Chen and F. A. Harrison are with the California Institute of Technology, Pasadena, California 91125. W. W. Craig is with the Lawrence Livermore National Laboratory, Livermore, California 94550.

Received 11 August 2002; revised manuscript received 29 October 2002.

0003-6935/03/132415-07$15.00/0

We describe here our research directed at the development of new depth-graded multilayers specifically designed for use in the 100–200-keV energy band. Future satellite instruments based on this technology, such as the envisioned Hard X-ray Spectroscopic Imaging (HSI) mission,[5] will allow us to measure, for example, the time history of ^{56}Ni emission (158 keV) in type 1a supernovas, investigate particle acceleration sites in young supernova remnants, measure the nuclear continuum and cutoff in Seyfert 1 galaxies, and detect Compton backscatter radiation (170 keV) in galactic black-hole candidates.

Depth-graded x-ray multilayers consist of bilayers comprising material pairs selected for both their optical and their material properties, with a range of bilayer thicknesses chosen so as to reflect over a wide energy band; multilayers designed for use above 100 keV in particular contain hundreds to thousands of nanometer-scale bilayers having near-perfect interfaces so as to achieve optimal performance. The range of bilayer thicknesses d is dictated by Bragg's law, $n\lambda = 2d \sin\theta$, where λ is the photon wavelength, θ is the grazing-incidence angle, and n is the Bragg order (which is generally set equal to 1.) The peak reflectance attainable from an x-ray multilayer depends in practice on the effective reflection coefficient at each interface, determined by the optical constants of the materials and by the interface width σ that characterizes the degree of interface perfection: both interfacial roughness and interfacial diffuseness

contribute to σ and thus reduce the effective reflection coefficient at each interface. The loss in reflectance due to interface imperfections can be modeled[6] as $\tilde{w}(s) = \exp(-s^2\sigma^2/2)$ (i.e., assuming an error function interface profile), where $s = 4\pi \sin\theta/\lambda$. The effective reflection coefficient at each interface in the multilayer stack is computed as $r' = r\,\tilde{w}(s)$, where r is the Fresnel reflection coefficient for the case of a perfectly smooth and sharp interface (which depends in the usual way on the difference in the optical constants on either side of the interface[7]). The loss in reflectance due to interface imperfections thus can be large above 100 keV, even at grazing incidence, and so the interface widths must be minimized as much as possible. Multilayer material selection is generally driven therefore by the ability to produce stable layers having maximally smooth and sharp interfaces.

We have produced by magnetron sputtering both periodic and depth-graded x-ray multilayers comprising a promising new material combination, W/SiC. We have determined interface widths and characterized the temporal and thermal stability of these films using x-ray reflectometry (XRR) measurements made at $E = 8$ keV. We have compared the results obtained for W/SiC films with those found for W/Si and W/B_4C multilayers, which have been investigated previously.[8–11] These results are described in Sections 2 and 3. We have also measured the hard x-ray reflectance of depth-graded W/SiC and W/Si films using synchrotron radiation in the range $E =$ 120–180 keV, as described in Section 4.

An important remaining difficulty with regard to the design and development of new hard x-ray multilayers is the lack of reliable optical data for candidate multilayer materials. The optical constants of the materials dictate the optical contrast at each interface (in accord with the Fresnel formalism just outlined), as well as the maximum useful number of bilayers that can be used (which is limited by absorption.) However, at x-ray energies above 100 keV, incoherent (Compton) scattering becomes important for most materials, yet there is little, if any, accurate experimental optical data available that would include incoherent scattering. Consequently, we have also prepared single-layer films of the candidate multilayer materials W, SiC, $Ni_{.93}V_{.07}$ (a nonmagnetic Ni alloy), and B_4C and made reflectance versus incidence angle measurements in the energy range $E =$ 120–180 keV to derive optical constants for these materials. These results are described in Section 5. Finally, we conclude in Section 6 with a summary of our results and a discussion of their significance with regard to the eventual development of a hard x-ray nuclear line telescope.

2. Sample Preparation

All the films described here were prepared by magnetron sputtering using a deposition system that has been described previously.[12] Films were deposited onto either polished Si (100) wafer segments measuring 1 cm × 1 cm or, in the case of films used for synchrotron measurements, onto superpolished glass substrates[13] measuring 1 cm thick by 76 mm in diameter. The background pressure in the vacuum chamber prior to deposition was less than 1×10^{-6} Torr in all cases, and the sputter gas (argon) pressure was maintained at 1.50 ± 0.01 mTorr during growth. The deposition rates, shown in Table 1, were determined from XRR measurements, and individual layer thicknesses in subsequent multilayer depositions were controlled by varying the rotation rate of the substrate over each magnetron cathode.

Table 1. Deposition Rates Determined from XRR

Material	Cathode Power (w)	Deposition Rate (nm/s)
W	300	0.37
SiC	500	0.14
Si	500	0.42
$Ni_{.93}V_{.07}$	200	0.26
B_4C	500	0.063

3. Low-Energy X-Ray Characterization

Periodic W/SiC multilayers containing $N = 300$ bilayers, with periods in the range $d = 2.15$–0.65 nm, were deposited as described above. The relative W-layer thickness was fixed at $\Gamma = d_w/d = 0.4$ in all cases. XRR measurements were made with a four-circle x-ray diffractometer having a sealed-tube Cu source and a Ge (111) crystal monochromator tuned to the Cu Kα line ($\lambda = 0.154$ nm, $E = 8.04$ keV). The angular resolution of this system is estimated to be δθ~0.015°. The XRR results are shown in Fig. 1. All films show relatively sharp Bragg peaks, indicating good stability during deposition.

Fits to the XRR data, made with the IMD software package,[14] were used to infer apparent interface widths σ, which are summarized in Table 2. For the two structures having $d > 1.8$ nm, interface widths $\sigma = 0.23$ nm were obtained, representing to our knowledge the smallest interface widths ever re-

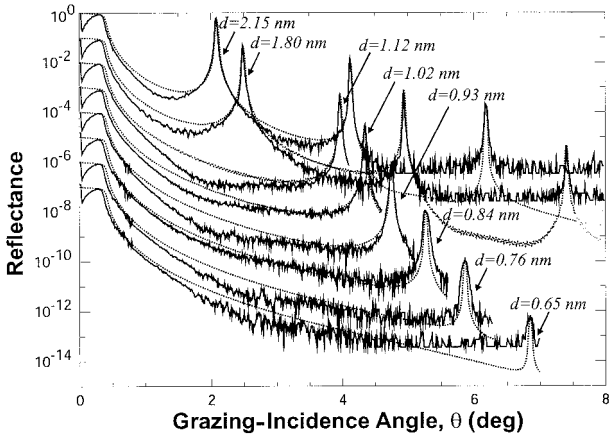

Fig. 1. XRR measurements of periodic W/SiC multilayers containing $N = 300$ bilayers, with periods d as indicated. For clarity, each curve is offset by a factor of 10 from the previous curve. Fits to the measured data are shown as dotted lines.

Table 2. Interface Widths Determined from the Fits to the XRR Data Shown in Fig. 1

Period d (nm)	Interface Width σ (nm)
2.15	0.23
1.80	0.23
1.12	0.30
1.02	0.30
0.93	0.30
0.84	0.33
0.76	0.34
0.65	0.34

ported. (In comparison, the interface widths for similar W/Si films were found previously to be $\sigma \sim 0.3$ nm.[10]) For structures having periods smaller than $d = 1.12$ nm, the interface widths gradually increase to 0.34 nm.

The XRR results for a depth-graded W/SiC multilayer (deposited onto a superpolished glass substrate) having $N = 1100$ bilayers are shown in Fig. 2(a). The W-layer thickness follows the power-law distribution

$$d_i = \frac{10.8435}{(49.4952 + i)^{0.055}}, \quad i = 1, \ldots 1100,$$

where $i = 1$ corresponds to the topmost W layer. The fractional W-layer thickness is again fixed at $\Gamma = 0.4$, so that the bilayer thickness ranges from $d_{\min} = 1.766$ nm to $d_{\max} = 2.098$ nm in this structure. The total film thickness is $t = 2.04$ μm. The fit to the XRR data [dotted line in Fig. 2(a)] corresponds to an interface width $\sigma = 0.26$ nm.

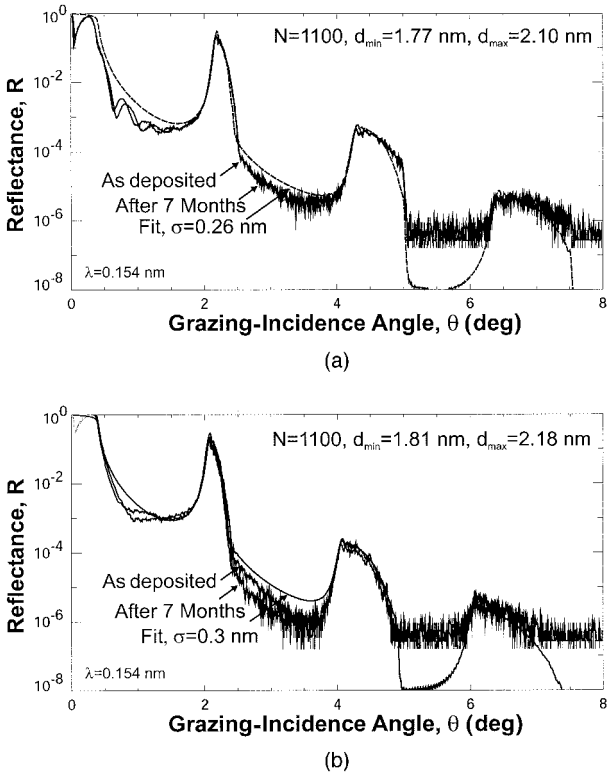

Fig. 2. XRR results for (a) depth-graded W/SiC and (b) W/Si multilayers, as described in the text.

The XRR data for a depth-graded multilayer similar to the one shown in Fig 2(a), but containing 1100 bilayers of W/Si, are shown in Fig. 2(b) for comparison. In this case the interface widths were found to be $\sigma = 0.30$ nm.

Both the W/SiC and the W/Si multilayers shown in Fig. 2 were found to be stable over time. Figures 2(a) and 2(b) show XRR measurements made the day after deposition as well as those made after seven months storage in air, and the two measurements are nearly identical in both cases. (There is a slightly greater difference, however, between the two measurements in the case of the W/Si film; the slight change in the W/Si film over time may be due to increased interface diffusion relative to the W/SiC film.)

In addition to the W/SiC and W/Si films shown in Fig. 2, we also grew a comparable depth-graded W/B_4C multilayer. The feasibility of using ultrashort-period W/B_4C films for use as normal-incidence reflective coatings in the soft x-ray band has been recently demonstrated, and these periodic structures were found to be stable over time.[11] However, in the case of the (much thicker) depth-graded structure investigated here, although the film initially had good x-ray reflectance, with interface widths $\sigma \sim 0.30$ nm, the film ultimately proved to be unstable over time and crazed from the substrate after several months, presumably as a result of high stress.

The thermal stability of a periodic W/SiC multilayer ($N = 300$, $d = 1.80$ nm) was measured and compared with that of a similar W/Si film ($N = 300$, $d = 1.74$ nm). The XRR data in Fig. 3 show the reflectance of as-deposited films compared with those annealed in air for 1 h at 100 °C and 300 °C. Neither the W/SiC nor the W/Si film revealed any significant changes after the 100 °C anneal. In the case of the 300 °C anneal, however, the peak reflectance of the first Bragg peak for the W/SiC film [Fig. 3(a)] was found to increase from 42 to 56%, with no discernable change in period, whereas the W/Si film [Fig. 3(b)] showed a decrease in peak reflectance from 33 to 13%, and a 1.5% reduction in period was observed.

4. High-Energy X-Ray Characterization

Hard x-ray reflectance measurements were made at beamline ID15A at the European Synchrotron Radiation Facility. A bent, double-crystal Laue monochromator using Si (311) reflections was configured to scan over the energy range from $E = 120$ to 180 keV. The monochromatic beam passed through two 130-mm-long W blocks separated by a 5-μm gap, thus providing collimation with $\delta\theta \sim 0.002°$ divergence. A two-circle diffractometer was constructed as follows: samples were placed on a precision rotation stage, and a Ge detector was mounted on a translation stage located 1.6 m from the sample; the translation stage was calibrated to act as a 2θ rotation stage. The Ge detector was used to measure the intensity of the

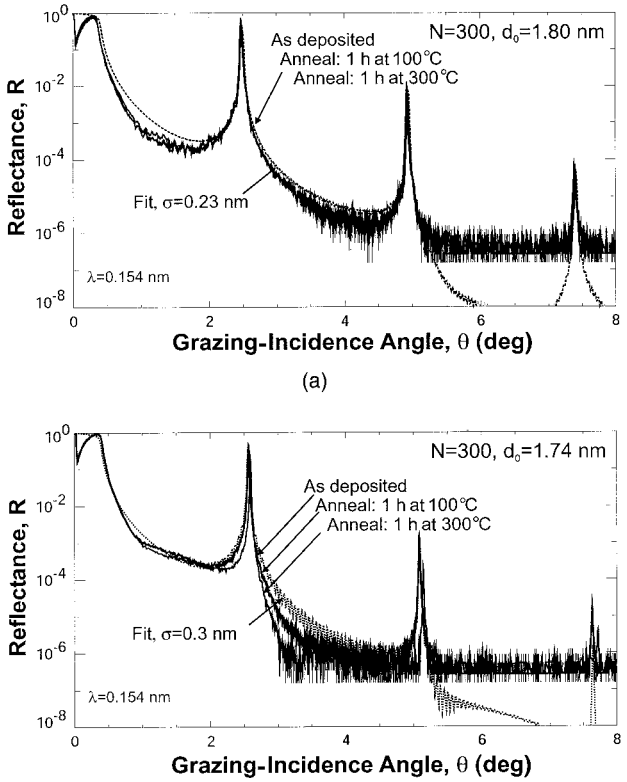

Fig. 3. XRR results for (a) periodic W/SiC and (b) W/Si multilayers comparing the as-deposited films with those annealed for 1 h at 100 °C and 300 °C.

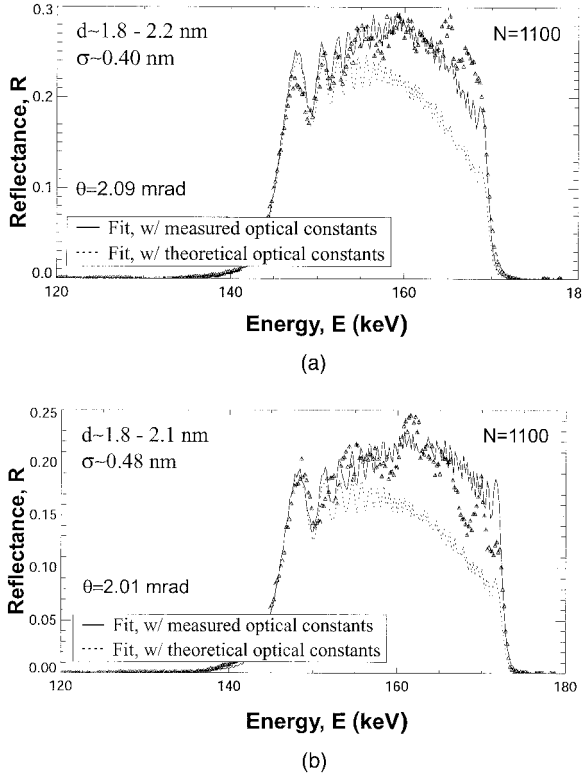

Fig. 4. Hard x-ray reflectance of (a) depth-graded W/SiC and (b) W/Si multilayers measured using synchrotron radiation. The solid lines are calculations made with experimentally determined optical constants, and the dotted lines are calculations made with theoretical optical constants, as described in Section 5.

straight-through and reflected beam. A second I_0 monitor detector was used to account for any drift in the incident flux, and the dark currents from both detectors were measured and subtracted from all intensity measurements. The absolute energy scale of the monochromator was determined by measurement of the angular position of the (111) reflection from an Al powder sample in the diffractometer. Reflectance measurements could be made either with fixed graze angles as a function of energy or with fixed energies as a function of graze angle over the range of $\theta \sim 0.01°–0.2°$.

The hard x-ray reflectance curves of the depth-graded W/SiC and W/Si multilayers described above (i.e., Fig 2.) are shown in Fig. 4, measured as a function of energy at $\theta = 0.12°$ for W/SiC and at $\theta = 0.115°$ for W/Si; the small difference in graze angles as presented in Fig. 4 was selected so that the reflectance profiles of the two samples (which have slightly different bilayer distributions, as indicated in Fig. 4) more closely overlap. The x-ray reflectance for the W/SiC film ranges from 17 to 29% over the energy band from $E = 146$ to 168 keV; the average reflectance is 25% as calculated over this same energy range. In comparison, the x-ray reflectance for the W/Si film is significantly lower (in spite of the slightly smaller graze angle), ranging from 12 to 26% over the energy band from $E = 147$ to 172 keV, with an average reflectance of 19%. The difference in hard x-ray reflectance between the two films is qualitatively consistent with the difference in interface widths determined from 8-keV XRR measurements.

The solid line in Fig. 4(a) is the calculated reflectance of the W/SiC film using the layer thickness distribution determined from XRR [Fig. 2(a)], the experimentally derived optical constants for W and SiC discussed in Section 5, and interface widths $\sigma = 0.4$ nm. The solid line in Fig. 4(b) is the calculated reflectance using the XRR layer thickness distribution, the experimentally derived optical constants for W, and interface widths $\sigma = 0.48$ nm. Because high-energy optical constants were not determined for Si, in this calculation we use optical constants for Si computed from atomic scattering factors and mass absorption coefficients that include incoherent scattering, as we describe in Section 5. In any case, both calculations are reasonably close to the measured curves. We discuss the significance of the larger (i.e., as compared with the XRR results) interface widths in Section 6.

5. High-Energy Optical Constants

X-ray reflectance versus graze-angle measurements were made over the energy range $E \sim 120–180$ keV, in 2-keV increments, for each of the four single-layer films mentioned above, i.e., W, SiC, $Ni_{.93}V_{.07}$, and

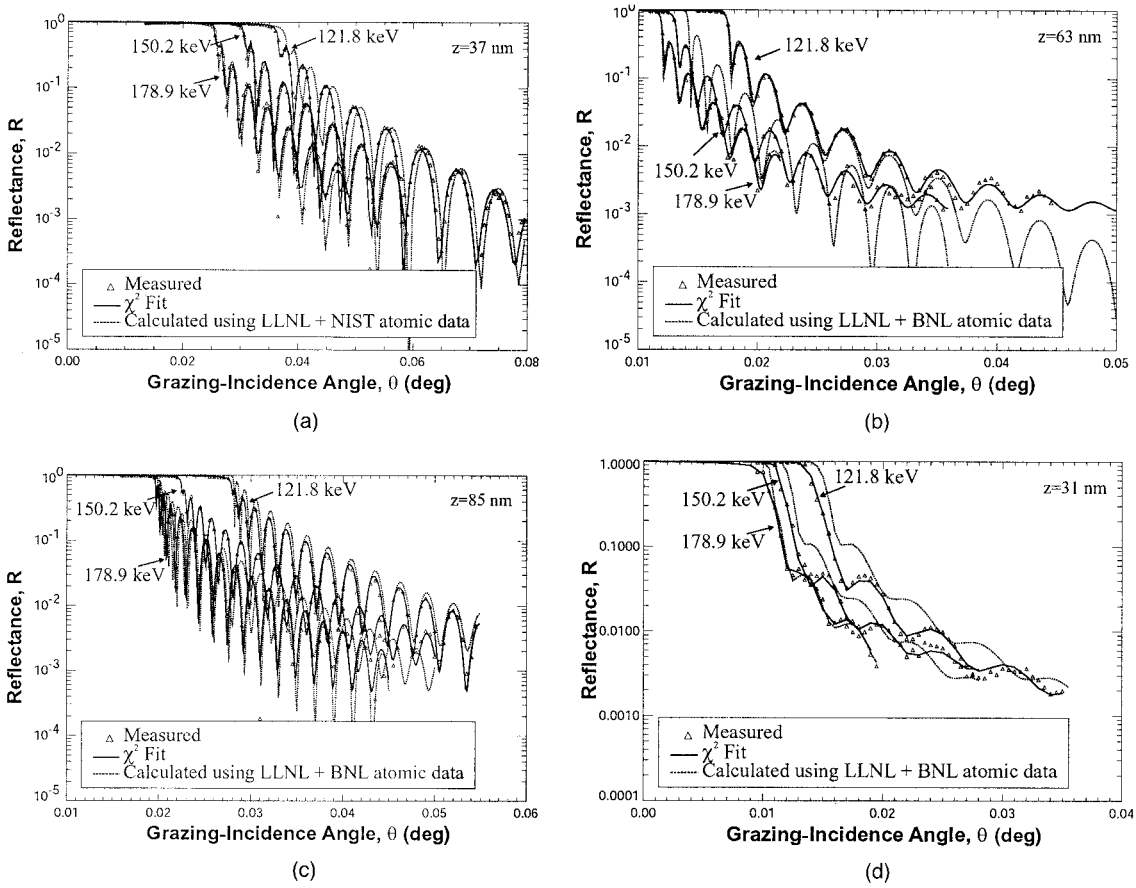

Fig. 5. X-ray reflectance versus graze-angle curves for single-layer films of (a) W, (b) SiC, (c) $Ni_{.93}V_{.07}$, and (d) B_4C. The film thicknesses determined from XRR are indicated in each case. Curves obtained at E = 121.8, 150.2, and 178.9 keV are indicated. χ^2 minimization fits to the measured data are shown as solid lines. The dotted lines are the reflectance curves calculated with optical constants computed from theoretical atomic scattering factors and mass absorption coefficients that account for incoherent scattering. (LLNL: Lawrence Livermore National Laboratory; NIST: National Institute of Standards and Technology; BNL: Brookhaven National Laboratory.)

B_4C, in order to derive optical constants for these materials. Measurements were made over 3–3.5 orders of magnitude in intensity, starting from graze angles below the critical angle for total external reflection in all cases (although the B_4C measurements are marginal at the highest energies). Typical reflectance (R-θ) curves are shown in Fig. 5.

We performed nonlinear, least-squares χ^2 minimization fits to the R-θ curves using IMD, with the optical constants (1-n) and k set as fit parameters; the best-fit curves to the example data shown in Fig. 5 are plotted as solid lines. A number of other fit parameters were used in addition to (1-n, k) to produce acceptable fits to the data, including the film thickness and surface roughness. Because of the large x-ray transparency of these materials above 120 keV, the fits are also sensitive to the optical constants of the underlying SiO_2 substrate. However, accurate optical constants for SiO_2 are not available in this energy range, and so we computed the substrate optical constants from the atomic scattering factors for Si and O and by setting the SiO_2 density as another fit parameter, thus approximating, albeit crudely, a mechanism to adjust the SiO_2 optical constants so as to adequately fit the reflectance curves.

The values of (1-n) and k for W, SiC, $Ni_{.93}V_{.07}$, and B_4C determined from the R-θ data are plotted in Fig. 6. The scatter in the derived values illustrates the precision with which these data have been determined. The solid lines in Fig. 6 are polynomial fits to the best-fit values, and these smooth curves were used to calculate the multilayer reflectance curves shown in Fig. 4.

Also shown in Fig. 6 as dotted lines are optical constants computed from a combination of theoretical atomic scattering factors[15] that do not include incoherent scattering and theoretical mass absorption coefficients[16] that do include incoherent scattering. In this case, the optical constants (n,k) were computed from the atomic scattering factors (f_1,f_2) in the usual way,[17] assuming bulk material densities ρ, but the values of the extinction coefficient k were simply replaced with those determined from the mass absorption coefficient μ according to $k = \mu\rho\lambda/4\pi$. Calculated reflectance curves computed from these theoretical optical constants are also shown as dotted lines in Figs. 4 and 5. These theoretical optical con-

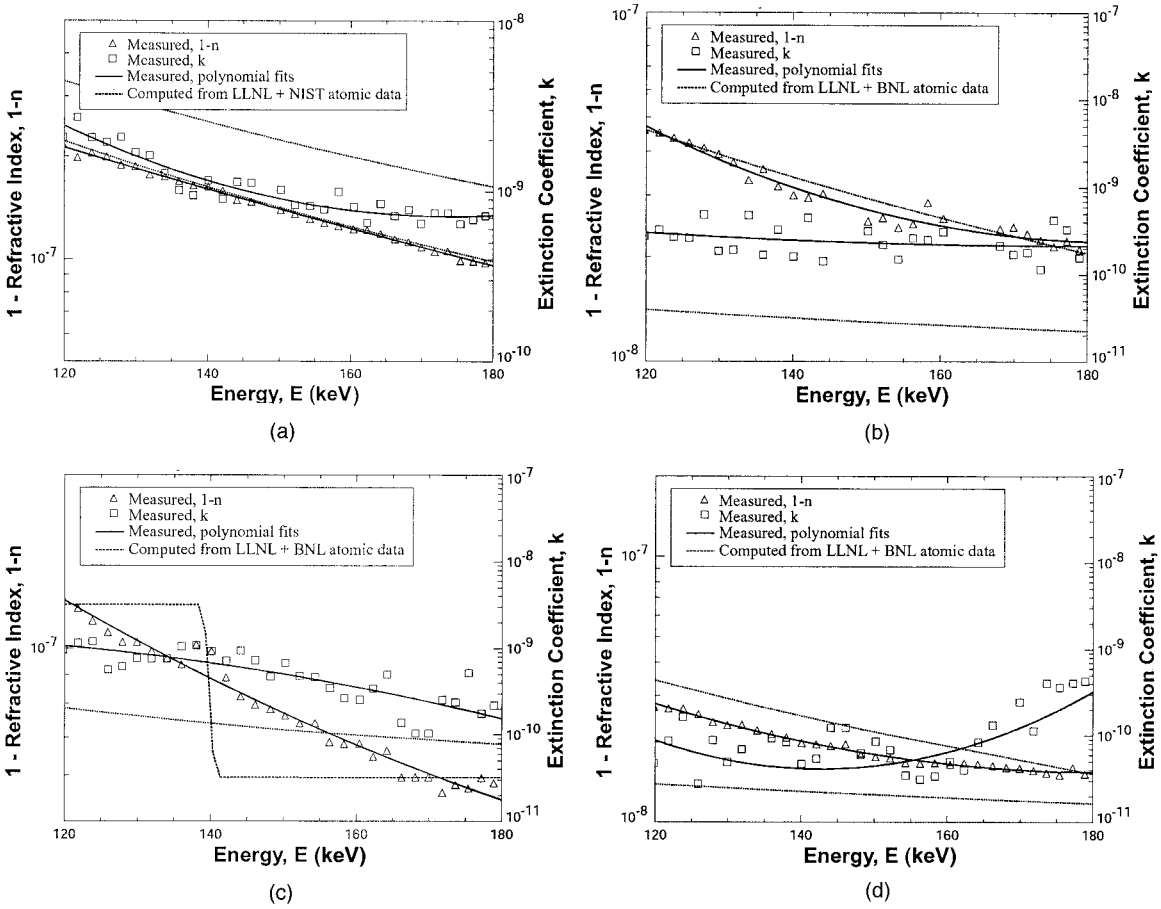

Fig. 6. Optical constants (1-n) (triangles) and k (squares) derived from reflectance versus incidence angle data for (a) W, (b) SiC, (c) $Ni_{.93}V_{.07}$, and (d) B_4C. The solid lines are polynomial fits to the experimental data. The dotted lines are theoretical values computed from atomic scattering factors and mass absorption coefficients, as described in the text. (LLNL: Lawrence Livermore National Laboratory; NIST: National Institute of Standards and Technology; BNL: Brookhaven National Laboratory.)

stants, as well as the calculated reflectance curves, deviate significantly from the experimental data, which is not surprising in light of the nonrigorous computational approach used to derive the theoretical values as just outlined.

6. Conclusion

We have produced by magnetron sputtering both periodic and depth-graded x-ray multilayers comprising a new material combination, W/SiC. Periodic structures containing $N = 300$ bilayers with periods in the range $d = 2.2–0.65$ nm were found to have interface widths $\sigma = 0.23$ nm for periods greater than $d \sim 1.7$ nm, gradually increasing to $\sigma \sim 0.34$ nm for $d = 0.65$ nm, as determined from XRR ($E = 8$ keV). Depth-graded structures containing $N = 1100$ bilayers, with periods in the range $d = 2.1–1.8$ nm, designed for use as broadband grazing-incidence x-ray mirror coatings operating in the range $E \sim 150–170$ keV at an incidence angle of $\theta \sim 2$ mrad were found from 8-keV reflectance measurements to have interface widths $\sigma \sim 0.26$ nm. We have also produced similar depth-graded structures comprising both W/Si and W/B_4C bilayers for comparison: both structures were found to have interface widths $\sigma \sim 0.30$ nm. The long-term stability of the W/SiC and W/Si films was found to be acceptable, with little change after seven months storage in air; however, the W/B_4C film was unstable and had crazed after four months. The thermal stability of periodic W/SiC and W/Si films ($N = 300$, $d \sim 1.7$ nm) was also measured: after a 1-h anneal at 300 °C, in the case of the W/SiC film, we measured an increase in the first-order peak reflectance (8 keV) from 42 to 56% with no discernable change in period, whereas the W/Si film showed a decrease in peak reflectance from 33 to 13% and a 1.5% change in period.

We measured the hard x-ray reflectance of the W/SiC and W/Si depth-graded structures using synchrotron radiation in the range $E = 120–180$ keV and found that the W/SiC film had significantly greater reflectance, in accord with the smaller interface widths determined from low-energy XRR measurements. However, the interface widths that best fit the hard x-ray multilayer data ($\sigma = 0.4$ nm for W/SiC, $\sigma = 0.48$ nm for W/Si) are significantly greater than those determined from 8-keV measurements ($\sigma = 0.26$ nm for W/SiC, $\sigma = 0.30$ nm for W/Si), suggesting that the interfacial roughness in these films is greater at the higher spatial frequen-

cies to which the hard x-ray measurements are sensitive.[18] (We note, however, that the interface width ratio between W/SiC and W/Si remains constant, approximately). The increase in σ might be due to propagated roughness emanating from the superpolished glass substrate, rather than high-frequency interfacial roughness intrinsic to the films: we plan to perform additional investigations in the future to identify the source of this apparent roughness increase.

We also made hard x-ray reflectance versus incidence angle measurements in this same energy range of thin films of W, SiC, $Ni_{.93}V_{.07}$, and B_4C—all candidate hard x-ray multilayer materials—in order to derive optical constants for these materials. In all cases, the experimental optical constants depart significantly from those computed from atomic scattering factors and mass absorption coefficients that include incoherent scattering, illustrating the importance of making experimental determinations of these quantities.[19] In any case, we have used the new optical constants for W and SiC to better fit the multilayer data. Future research will be directed at measurements of the optical constants of other candidate multilayer materials as well.

The measured hard x-ray performance of the depth-graded multilayers designed for use in the 150–170-keV band, shown in Fig. 4, demonstrates the technical feasibility of use of this thin-film coating technology for the development of a hard x-ray nuclear line telescope operating in this energy range. Further reductions in multilayer interface widths, coupled with ongoing research directed at the development of high-quality, lightweight mirror substrates having low surface roughness, should lead to even better performance in the future. Furthermore, with the availability of experimentally determined optical constants, such as those described here, we can now hope to produce truly optimized depth-graded multilayer designs, perhaps by use of lighter elements (such as $Ni_{.93}V_{.07}$) that have lower absorption and thus the potential for even higher reflectance in this energy range.

This research was funded by a Supporting Research and Technology grant from NASA.

References and Notes

1. C. J. Hailey, S. Abdali, F. E. Christensen, W. W. Craig, T. R. Decker, F. A. Harrison, and M. Jimenez-Garate, "Substrates and mounting techniques for the High-Energy Focusing Telescope (HEFT)," in *EUV, X-Ray and Gamma-Ray Instrumentation for Astronomy VIII*, O. H. Siegmund and M. A. Gummin, eds., Proc. SPIE **3114,** 535–544 (1997).
2. K. Yamashita, P. J. Serlemitsos, J. Tueller, S. D. Barthelmy, L. M. Bartlett, K. W. Chan, A. Furuzawa, N. Gehrels, K. Haga, H. Kunieda, P. Kurczynski, G. Lodha, N. Nakajo, N. Nakamura, Y. Namba, Y. Okajima, D. Palmer, A. Parsons, Y. Soong, S. M. Stahl, H. Takata, K. Tamura, Y. Tawara, and B. J. Teegarden, "Supermirror hard x-ray telescope," Appl. Opt. **37,** 8067–8073 (1998).
3. H. Tananbaum, N. White, and P. Sullivan, eds., *Proceedings of the High Throughput X-Ray Spectroscopy Workshop* (Harvard–Smithsonian Center for Astrophysics, Cambridge, Mass., 1996).
4. See, for example, J. Koglin, H. C. Chen, F. E. Christensen, J. Chonko, W. W. Craig, T. R. Decker, M. A. Jimenez-Garate, C. J. Hailey, F. A. Harrison, C. P. Jensen, M. Sileo, D. L. Windt, H. Yu, "Development and production of hard x-ray multilayer optics for HEFT," in *X-Ray and Gamma-Ray Telescopes and Instruments for Astronomy*, J. E. Truemper and H. D. Tananbaum, eds., Proc. SPIE (to be published).
5. F. A. Harrison, S. E. Boggs, H. C. Chen, F. E. Christensen, W. W. Craig, N. A. Gehrels, J. E. Grindlay, C. J. Hailey, P. Pinto, S. Thorsett, J. Tueller, and S. E. Woosley, "High-resolution spectroscopic imaging mission (HSI)," in *X-Ray and Gamma-Ray Telescopes and Instruments for Astronomy*, J. E. Truemper and H. D. Tananbaum, eds., Proc. SPIE (to be published).
6. D. G. Stearns, "The scattering of X-rays from non-ideal multilayer structures," J. Appl. Phys. **65,** 491–506 (1989).
7. J. D. Jackson, *Classical Electrodynamics*, 2nd ed. (Wiley, New York, 1975), pp. 281–282.
8. P. Høghøj, E. Ziegler, J. Susini, A. Freund, K. D. Joensen, and P. Gorenstein, "Broadband focusing of hard X-rays using a supermirror," in *Physics of X-Ray Multilayer Structures*, Vol. 6 of 1994 OSA Technical Digest Series (Optical Society of America, Washington, D.C., 1994), pp. 142–145.
9. P. H. Mao, F. A. Harrison, Y. Y. Platonov, D. Broadway, B. Degroot, F. E. Christensen, W. W. Craig, and C. J. Hailey, "Development of grazing incidence multilayer mirrors for hard x-ray focusing telescopes," in *EUV, X-Ray and Gamma-Ray Instrumentation for Astronomy VIII*, O. H. Siegmund and M. A. Gummin, eds., Proc. SPIE **3114,** 526–534 (1997).
10. D. L. Windt, F. E. Christensen, W. W. Craig, C. Hailey, F. A. Harrison, M. Jimenez-Garate, R. Kalyanaraman, and P. H. Mao, "Growth, structure and performance of depth-graded W/Si multilayers for hard X-ray optics," J. Appl. Phys **88,** 460–470 (2000).
11. D. L. Windt, E. M. Gullikson, and C. C. Walton, 'Normal-incidence reflectance of optimized W/B_4C x-ray multilayers in the range 1.4 nm $< \lambda <$ 2.4 nm," Opt. Lett. **27,** 2212–2214 (2002).
12. D. L. Windt and W. K. Waskiewicz, "Multilayer facilities required for extreme-ultraviolet lithography," J. Vac. Sci. Technol. B **12,** 3826–3832 (1994).
13. Glass substrates were provided by Wave Precision, Moorpark, Calif.
14. D. L. Windt, "IMD—software for modeling the optical properties of multilayer films," Comput. Phys. **12,** 360–370 (1998).
15. High-energy atomic scattering factors are available at http://www-phys.llnl.gov/Research/scattering/asf.html.
16. High-energy mass absorption coefficients are available for elements at http://physics.nist.gov/PhysRefData/XrayMassCoef/cover.html. For compounds, see http://bnlnd2.dne.bnl.gov/.
17. B. L. Henke, E. M. Gullikson, and J. C. Davis, "X-ray interactions: photoabsorption, scattering, transmission, and reflection at E = 50–30,000 eV, Z = 1–92," At. Data Nucl. Data Tables **54,** 181–342 (1993).
18. D. L. Windt, W. K. Waskiewicz, and J. E. Griffith, "Surface finish requirements for soft x-ray mirrors," Appl. Opt. **33,** 2025–2031 (1994).
19. The optical constants that we derived here will be included with the next release of IMD, available at http://cletus.phys.columbia.edu/windt/imd.